

# Simulation and structural parameter optimization of rotary blade cutting soil based on SPH method

Xiongye Zhang<sup>1,3</sup>, Xue Hu<sup>1,3,4</sup>, Lixin Zhang<sup>1,2,3,4\*</sup>, Abdalla Noureldin Osman Kheiry<sup>5</sup>

(1. College of Mechanical and Electrical Engineering, Shihezi University, Shihezi 832000, Xinjiang, China;

2. Bingtuan Energy Development Institute, Shihezi University, Shihezi 832000, Xinjiang, China;

3. Xinjiang Production and Construction Corps Key Laboratory of Modern Agricultural Machinery, Shihezi 832000, Xinjiang, China;

4. Key Laboratory of Northwest Agricultural Equipment, Ministry of Agriculture and Rural Affairs, Shihezi 832000, Xinjiang, China;

5. College of Agricultural Engineering, Sudan University of Science and Technology, Khartoum 999129, Sudan)

**Abstract:** Pre-sowing mechanical tillage in crop fields is a primary task and important aspect of crop production. The interaction between the tillage components and the soil plays a crucial role in determining the energy consumption of tillage machinery. Therefore, it is essential to investigate soil-tool interaction mechanisms and optimize tool design for energy savings in soil cutting. The study employed the Smoothed Particle Hydrodynamics (SPH) method to investigate the soil cutting process of a typical rotary blade. The article describes the principles and modeling process of the SPH method in detail. It includes the selection of constitutive models, boundary treatments, and particle conversion. A high-precision soil-tool interaction model was established to analyze the deformation zone of the soil, cutting energy, cutting resistance, and soil particle movement. Orthogonal simulation experiments and response surface methodology were used to optimize key design parameters of the rotary blade considering both the reduction in cutting power consumption and the impact on the structural performance of the tool. The optimal parameters were determined as follows: a bending point included angle of 30°, a side cutting edge bending line direction angle of 51°, and a bending angle of 120°. These parameters resulted in a minimum power consumption of 0.181 kW while meeting the required structural performance. Finally, experiments were conducted on field rotary tillage, and the measured power consumption showed a deviation of 7.1% from the simulated power consumption. The optimized power consumption was reduced by 9.52% compared to the initial power consumption, validating the accuracy of the simulation process and the effectiveness of energy savings.

**Keywords:** rotary blade, Smoothed Particle Hydrodynamics, response surface methodology, energy consumption optimization

**DOI:** [10.25165/ij.ijabe.20241703.8470](https://doi.org/10.25165/ij.ijabe.20241703.8470)

**Citation:** Zhang X Y, Hu X, Zhang L X, Kheiry A N O. Simulation and structural parameter optimization of rotary blade cutting soil based on SPH method. *Int J Agric & Biol Eng*, 2024; 17(3): 82–90.

## 1 Introduction

Xinjiang is one of the largest crop-planting regions in the country. The level of modern agricultural mechanization has been increasing yearly<sup>[1]</sup>. Among them, mechanical tillage before sowing is a primary task and important link in crop production, significantly role in improving crop yield<sup>[2,3]</sup>. Among various tillage methods, rotary tillage is the most widely used. The operation occurs in the field and involves the soil<sup>[4]</sup>. The rotary blades, as the part that directly contacts the soil, often experience significant impact and loads during the soil cutting process, which can easily lead to structural bending and deformation, directly affecting its tillage effectiveness, work efficiency, and lifespan. In agricultural cultivation, energy demand is crucial for characterizing and evaluating operations<sup>[5]</sup>. The interaction between tillage components and the soil is a key determinant affecting the energy consumption of agricultural machinery. Therefore, researching the interactive processes between these components is of paramount importance.

The main methods for studying soil cutting processes include theoretical, experimental, and numerical simulation<sup>[6]</sup>. With the continuous development of computer technology, numerical simulation methods have demonstrated significant advantages in addressing soil cutting problems<sup>[7,8]</sup>, primarily encompassing Finite Element Method (FEM), Discrete Element Method (DEM), and Smoothed Particle Hydrodynamics (SPH). As a mesh-free approach, the SPH method effectively avoids grid distortion issues caused by large soil deformations in the FEM. It eliminates the cumbersome parameter calibration associated with the DEM<sup>[9]</sup>. In recent years, this method has garnered widespread attention from scholars globally. For example, Li et al.<sup>[10]</sup> utilized LS-DYNA to simulate the dynamic process of high-speed tool cutting soil, validating the reliability of the SPH method through on-site experiments. Sun et al.<sup>[11]</sup> established a cutting model for a furrow opener based on the SPH method, predicting power variations during cultivation. Scholars<sup>[12-14]</sup> employed the SPH method for the numerical simulation of soil cutting processes involving different agricultural machinery components, achieving satisfactory simulation and prediction results. To reduce the energy consumption in the interaction between tillage tools and soil, researchers primarily utilize parameter optimization, biomimetic design, and vibration reduction<sup>[15-17]</sup>. Among these, optimizing working or structural parameters is the most common approach. For instance, Zheng et al.<sup>[18]</sup> conducted DEM simulation experiments to reduce torque and increase soil shattering rate, optimizing a no-till seeder's trapezoidal straight knife structure. Using the SPH method,

**Received date:** 2023-11-30 **Accepted date:** 2024-05-20

**Biographies:** Xiongye Zhang, MS candidate, research interest: agricultural machinery equipment, Email: [1074485181@qq.com](mailto:1074485181@qq.com); Xue Hu, Associate Professor, research interest: new materials for agricultural machinery, Email: [huxue@foxmail.com](mailto:huxue@foxmail.com); Abdalla Noureldin Osman Kheiry, Professor, research interest: Agricultural engineering, Email: [20212309406@stu.shzu.edu.cn](mailto:20212309406@stu.shzu.edu.cn).

\*Corresponding author: Lixin Zhang, Professor, research interest: intelligent agricultural equipment. Shihezi University, No. 221 North Fourth Road, Shihezi City 83200, China. Tel: +86-18899596017, Email: [Zhix2001329@163.com](mailto:Zhix2001329@163.com).

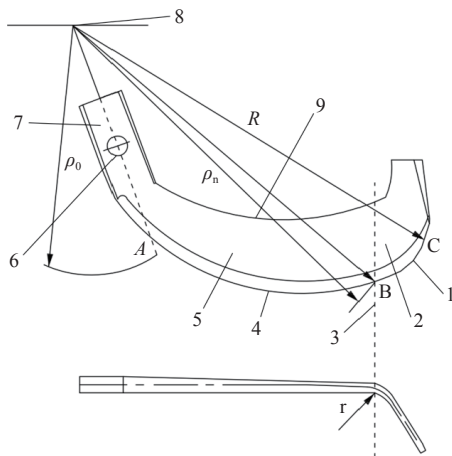
Jin et al.<sup>[19]</sup> conducted simulation experiments to study the influence of different cultivation parameters and structural parameters on ploughing performance. Some scholars such as Zhang et al.<sup>[20]</sup>, Wang et al.<sup>[21]</sup>, and Ma et al.<sup>[22]</sup>, focused on different tillage components (e.g., rotary blades, furrow openers, deep loosening shovels) and various operational scenarios, conducting corresponding parameter optimization studies through simulation and experimental methods. The aim is to reduce tillage resistance and energy consumption and improve overall tillage performance.

Based on the analysis of simulation and optimization methods, this study employs the SPH method to conduct simulation and optimization research on the soil-cutting process of a typical rotary tillage tool. The modelling process is explained in detail, establishing a mutual interaction model between the rotary tillage tool and the soil. Key cutting parameters are obtained, and the critical structural parameters are optimized utilizing the response surface optimization method to reduce soil cutting energy consumption. Finally, the simulation results are compared with actual working conditions to validate the effectiveness of the simulation and optimization. This study provides theoretical references and technical support for a deeper understanding of the interaction mechanisms between the tillage components and the soil and the energy-efficient design of other typical tillage equipment, such as disc harrows and Ploughshares.

## 2 Materials and SPH method

### 2.1 Structural modelling

As typical tillage components, rotary blades find extensive applications in various agricultural activities such as furrow opening, rotary cultivation, soil pulverization, and residue incorporation. The experiment selected the IT 245 standard rotary blade from the Dongfanghong 1GQK-125 model rotary tiller as the research subject. The blade was parametrically modelled based on GB/T 5669-2017 "Design of Rotary Tiller Blades and Holders"<sup>[23]</sup>. The schematic diagram of the rotary tillage blade structure is shown in Figure 1, and the range of critical structural parameters is presented in Table 1.



1. Tangent cutting edge 2. Front cutting part 3. Bend line 4. Side cutting edge 5. Side cutting part 6. Mounting hole 7. Tool shank 8. Rotation center of cutter roll 9. Back edge curve

Note:  $\rho_0$  is the starting radius of the side cutting edge, mm;  $R$  is the turning radius of the blade, mm;  $\rho_n$  is the radius of any point on the side cutting edge, mm;  $r$  is the bending radius of the normal cutting surface, mm;  $A$  is the position of the side cutting edge;  $B$  is the bending angle part;  $C$  is the tangent blade area

Figure 1 Schematic diagram of the rotary cutter curved blade structure

Table 1 Rotary tiller construction parameters range

Serial number	Parameters	Range of values	Value
1	Bending corner ( $\beta$ )	110°-130°	120°
2	Bend point wrap corner ( $\theta'$ )	24°-30°	27°
3	Angle between the end radius of side cutting edge and bend line ( $\alpha$ )	42°-52°	50°
4	Thickness ( $c_1$ )	3.5-5.5 mm	4 mm
5	Positive cutting face end blade height ( $h$ )	40-50 mm	45 mm
6	Working width ( $b$ )	35-45 mm	45 mm

By conducting soil-cutting simulation experiments and optimizing its structural parameters to reduce soil-cutting energy consumption, this study is expected to provide valuable guidance for optimizing the design of existing national standard rotary tillage blades and various types of rotary tillage blades, such as furrow openers and residue incorporation blades. Additionally, it has the potential to extract general design principles and insights, offering comprehensive theoretical foundations for the optimization design of different types of rotary tillage blades.

### 2.2 Force analysis

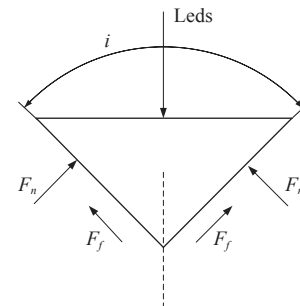
Rotary tilling involves the periodic cutting, turning, and throwing of a curved blade to till the soil. The primary forces acting on the blade during cutting include cutting resistance on the blade surface, normal and tangential forces on the blade edge, and frictional force generated when the blade surface cuts the soil. Soil resistance to the tool results in tool wear and power loss.

The rotary tiller blade tip is designed with a double-edged grinding blade form. As the blade edge moves vertically into the soil with an absolute speed  $v$ , soil particles slide towards the left and right blade surfaces due to the angle of blade edge grinding, denoted as  $i$ .

The force situation on the blade surface when cutting the soil is shown in Figure 2. The frictional force of the soil on the blade surface element  $ds$  can be expressed as:

$$dF = \frac{ELf ds}{f \cos \frac{i}{2} + \sin \frac{i}{2}} \quad (1)$$

where,  $ds$  is the area of soil microelements, mm<sup>2</sup>;  $dF$  is the frictional force of soil on the micro element  $ds$  of the cutting surface, N;  $f$  is the friction coefficient between soil and plow blade;  $E$  is the soil compressive strength, MPa;  $i$  is the angle of double grinding edge, (°);  $L$  is the width of blade surface, mm.



Note: Leds are the downward pressure of soil on the blade grinding angle  $i$ , N.

Figure 2 Schematic diagram of the forces on the cutter face cutting the soil

The resistance experienced by the curved blade of rotary tiller when cutting through the soil is shown in Figure 3. In the diagram, while the curved blade undergoes a counterclockwise rotational motion, it simultaneously moves horizontally from left to right. The shaded area represents the soil element in contact with the curved

blade, and the dashed line represents the trajectory of motion of the rotary tiller blade tip. As the blade moves, it continuously compresses the soil. Assuming that surface AB represents the soil's shear plane subjected to the cutting action of the curved blade at that particular moment when the shearing force exerted by the curved blade on the soil reaches the corresponding shear strength of the soil, the soil undergoes shear deformation and starts sliding along the surface in the direction indicated by AC. The tangential plane of the curved blade experiences both the frictional force  $F_f$ , and the normal force  $F_n$  from the soil, with the resultant force  $F_r$  being the vector sum of the two. On the shear plane, the soil experiences the shear force  $F_t$ , the normal force  $F_{sn}$ , and the resultant force  $F_{sr}$  has the same magnitude as  $F_r$  but acts in the opposite direction.

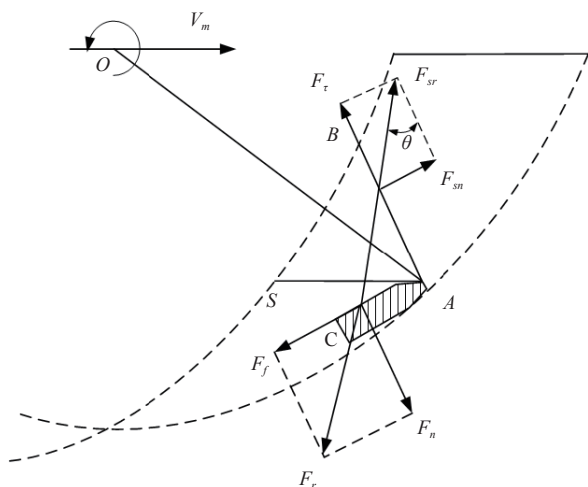
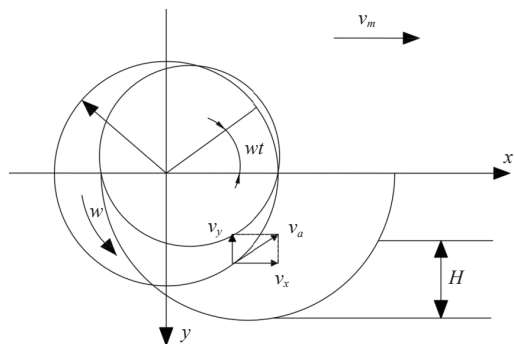


Figure 3 Schematic diagram of resistance to soil cutting by rotary cutter

**2.3 Motion analysis**

The motion of the rotary tillage blade during the soil cutting process primarily consists of two parts: On one hand, it moves forward along with the machine unit, and on the other hand, it undergoes high-speed rotational motion with the disc. The combined trajectory of these two motions is a trochoidal motion. A coordinate system is established with the axis of rotation as the origin, where the positive direction of the  $x$ -axis aligns with the forward direction, and the positive direction of the  $y$ -axis is set vertically downward, as shown in Figure 4. Assuming that the blade rotates clockwise, the equation for the motion trajectory of the blade endpoint is as follows<sup>[24]</sup>:



Note:  $v_m$  represents the forward speed, m/s;  $w$  represents the tool speed, rad/s;  $H$  represents the tillage depth, m;  $v_x$ ,  $v_y$ , and  $v_a$  are the horizontal and vertical separation and convergence velocities of the tool at that point, m/s.

Figure 4 Trajectory of rotary plow blade movement

$$\begin{cases} x = v_m t + R \cos \omega t \\ y = R \sin \omega t \end{cases} \quad (2)$$

where,  $R$  is the radius of gyration of the end point of the trenching cutter disc, m;  $t$  is time, s;  $v_m$  is the forward speed of the trencher, km/h;  $w$  is the angular speed of the cutter shaft, rad/s.

Let  $\lambda = v_p/v_m = wR/v_m$ , substituting  $\varphi = \omega t$  into the above equation, then obtained:

$$\begin{cases} x = R \left( \frac{\varphi}{\lambda} + \cos \varphi \right) \\ y = R \sin \varphi \end{cases} \quad (3)$$

**2.4 SPH method**

Compared to other simulation methods, the Smoothed Particle Hydrodynamics (SPH) method offers advantages in its ability to effectively handle free-surface fluid and solid boundary problems. Therefore, it can better capture the contact and deformation behavior between soil and cutting tools during simulating soil cutting processes. Additionally, because the SPH method is based on particles, it can more flexibly handle the heterogeneity and complex shapes of soil, which is very useful in simulating soil cutting processes. However, the SPH method also has some potential limitations, such as higher computational costs, requiring more computing resources and time. Furthermore, its accuracy and stability may be influenced by particle distribution and sampling density, so careful control of parameters is necessary during the simulation process to ensure the reliability of results. Below, the principles and simulation process will be detailed.

**2.4.1 SPH fundamentals**

The Smoothed Particle Hydrodynamics (SPH) algorithm is a pure Lagrangian method that does not use discretized units during computation. Instead, it utilizes moving points (particles or nodes) with fixed mass. The fundamental equations employed in SPH include conservation and constitutive equations for solid materials<sup>[25]</sup>. The SPH algorithm allows material interfaces and straightforwardly and accurately captures complex constitutive behaviors. It is particularly suitable for addressing the challenging problem of material fracture under high-rate loading conditions. The core of the SPH method lies in the interpolation theory. SPH represents the problem domain using a set of distributed particles and solves the domain using interpolation functions.

In SPH, an interaction force exists between particles, where the properties of a particle diffuse to its surrounding particles. This diffusion process is governed by a smoothing kernel function, which describes how the properties spread and attenuate with increasing distance. The "smoothing kernel radius" refers to the maximum radius within which the influence of a particle is considered significant. The concept of "smooth kernel" is also involved in the SPH algorithm, where the knowledge of the velocity and energy of any particle at any given time is required during the solving process, thus necessitating the introduction of a kernel function.

The field function undergoes a process of "smoothing" through the kernel function and is then integrated over the entire solution domain. This process yields the dynamic characteristic functions that represent each particle<sup>[26,27]</sup>:

$$\prod^h f(x) = \int f(y)W(x-y,h)dy \quad (4)$$

where,  $W$  is the kernel function and uses the auxiliary function  $\theta$  defined as:

$$W(x, h) = \frac{1}{h(x)^n} \theta(x) \quad (5)$$

where,  $V$  is the spatial dimension;  $h$  is the smooth length.  $W(x, h)$  is the spike function, and in this study, the cubic B-sample proposed by Monaghan et al.<sup>[28]</sup> was used, which takes the form:

$$\theta(\mu) = C \begin{cases} 1 - 1.5\mu^2 + 0.75\mu^3, & |\mu| \leq 1 \\ 0.25(2 - \mu)^3, & 1 \leq |\mu| \leq 2 \\ 0, & 2 \leq |\mu| \end{cases} \quad (6)$$

where,  $\mu$  is the relative distance between particles at  $x$  and  $y$ , with  $\mu = |x - y|/h$ ;  $C$  being a fixed coefficient, with  $C=1/h$ ,  $C=15/7nh^2$ ,  $C=3/2nh^3$  in one, two and three-dimensional problems, respectively.

An expression for the integral of the derivative of the function is obtained for Equation (9) as

$$\nabla f(x) = - \int f(y) \nabla W(x - y, h) dy \quad (7)$$

The smoothing length  $h$  affects both computational efficiency and accuracy. In the 1980s, Benz<sup>[29]</sup> introduced the concept of variable smoothing length to address the challenges posed by material expansion and compression. This concept ensures that there are a sufficient number of particles within the neighborhood of a particle, allowing for an effective approximation of continuous variables. Variable smoothing length refers to an increase in the smoothing length when particles separate, and a decrease in the smoothing length when particles converge. By allowing the smoothing length to vary, it ensures that the same number of particles are maintained within the neighborhood. Compared to a fixed smoothing length, variable smoothing length significantly improves computational speed and accuracy.

The smoothing length needs to be set with a maximum value and a minimum value, which are respectively 2 times and 0.2 times the initial smoothing length. These values are suitable for most problems, and the smoothing length varies between the maximum and minimum values.

$$h_{\min} h_0 < h < h_{\max} h_0 \quad (8)$$

where,  $h$  is the initial smooth length;  $h_{\max}$  and  $h_{\min}$  are coefficients, with a factor of 1;  $h_0$  is a fixed smooth length that does not vary with time or space.

#### 2.4.2 Boundary treatment

In the SPH algorithm, particles near or on the boundaries suffer from loss, leading to inaccurate integration and interpolation results near the boundaries. As an unstructured grid method, boundary handling in the SPH algorithm is relatively more challenging than grid-based numerical methods. In recent years, researchers have proposed various boundary handling methods for the SPH algorithm, such as the mirror particle method and virtual particle method, to address this issue.

In this study, the multi-layer boundary handling method, widely used in recent years, is adopted for the SPH simulation of soil cutting. This method involves placing multiple layers of virtual particles outside the computational domain. The outermost layer of virtual particles has the same density as the fundamental particles inside the domain, and their thickness and velocity remain constant with a velocity of 0. Therefore, the boundary particles do not move. The innermost layer of virtual particles represents the solid boundary and undergoes interpolation calculations along with the internal particles, as shown in Figure 5. This method of handling solid boundaries is effective in summation estimation, allowing a sufficient number of particles to be engaged in the interpolation

calculations, reducing computational errors and improving accuracy.

#### 2.4.3 Constitutive relationship model

The selection of soil constitutive relationships is crucial for the accuracy of the simulation results in soil cutting numerical simulations. The MAT147 (\*MAY\_FHWA\_SOLID) soil model material from LS-DYNA's material library is chosen to make the numerical simulation of tool cutting soil more realistic. The Drucker-Prager plastic model, which considers factors such as shear strain failure and viscoplasticity is utilized. The model is modified based on the Mohr-Coulomb yield criterion<sup>[30]</sup>. Before and after the modification, the yield surfaces are fitted with hyperbolic curves, as shown in Figure 6.

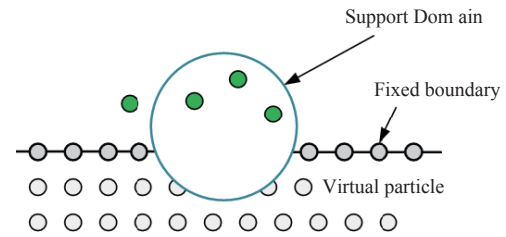


Figure 5 Multi-layer boundary treatment

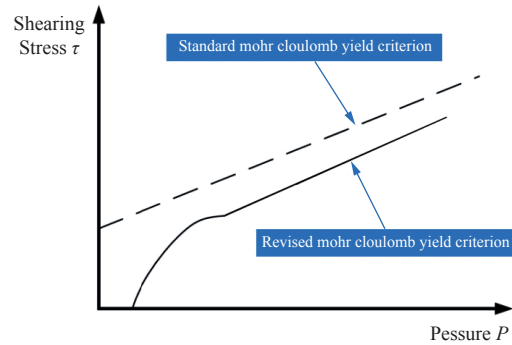


Figure 6 Modified Mohr-Coulomb yielding criterion

The modified Mohr-Coulomb yield criterion incorporates the effects of strain rate, moisture content, and element deletion, making the soil model more realistic. The yield surface of this model is represented as:

$$F = -P \sin \phi + \sqrt{J_2 K(\theta^2) + a \text{hyp}^2 \sin^2 \phi} - c \cos \phi = 0 \quad (9)$$

where,  $P$  is the pressure, Pa;  $\phi$  is the angle of internal friction, ( $^\circ$ );  $J_2$  is the 2nd invariant of the pressure deflection tensor;  $K(\theta^2)$  is a function of the tensor plane angle;  $c$  is the cohesive force, N;  $a \text{hyp}$  is the modified Mohr-Coulomb yielding criterion for yield surface similarity.

The soil density  $\rho$  measured by the ring-cut method and the soil moisture content measured by the drying method; the soil elastic modulus  $E$  and Poisson's ratio  $\nu$  determined by the soil triaxial test, so the shear modulus  $G$  can be known from the equation:  $G = E/2(1 + \nu)$ ; the cohesion coefficient  $C$  and internal friction angle  $\phi$  determined by the soil density and moisture content, and the yield surface coefficient obtained from the equation, the soil model material parameters are listed in Table 2.

#### 2.4.4 Modelling process

The specific process of combining the Finite Element Method (FEM) with the Smoothed Particle Hydrodynamics (SPH) method for simulating the cutting of soil by a rotary tillage blade is shown in Figure 7. It involves the following steps:

- 1) Save the established 3D model of the rotary tillage blade as a

**Table 2 Soil material parameters**

Parameters	Value	Parameters	Value
Soil density/(g·mm <sup>-3</sup> )	2.35e+04	Shear modulus/MPa	0.2e+8
Relative density of soil particles/(g·mm <sup>-3</sup> )	2.68	Moisture content/%	10.64
Water density/(g·mm <sup>-3</sup> )	1.0e+03	Angle of internal friction/(°)	0.436
Bulk modulus/MPa	0.35e+8	Modified yield surface factor	9.7e+3
Viscoplasticity parameters	1.1	Internal Cohesion/MPa	32.5

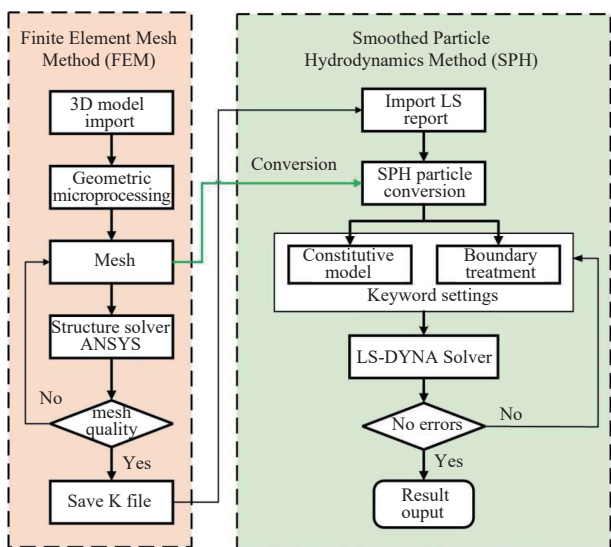


Figure 7 FEM-SPH coupling simulation flow

STEP file and import it into ANSYS. Apply filleting to some regions of the blade to ensure smoother transitions. To simplify the computation and improve the quality of the mesh, remove complex components such as bolts, nuts, and washers;

2) Use solid elements to mesh the tool. The blade portion is divided into 3257 elements. Verify the quality of the mesh and save it as a K file;

3) Import the K file into the LS-PrePost software. Convert the mesh into SPH particles using the SPH algorithm and set critical parameters such as boundary conditions and constitutive models. This step is one of the most crucial for the SPH method;

4) After the settings are completed, use the LS-DYNA solver to simulate and examine the results and data.

The finite element mesh model of the soil is imported into the LS-PrePost software, and the nodes of the finite element model are converted into SPH particles. During the conversion process, it is ensured that the number of particles generated is the same as the number of nodes in the mesh. The conversion result is shown in Figure 8.

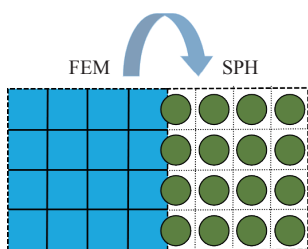


Figure 8 Schematic diagram of node conversion

The following keywords are added: The soil constitutive model \*MAT147 and the tool material model \*MAT\_RIGID; The point-to-surface contact \*AUTOMATIC\_NODES\_TO\_SURFACE is used for the contact between the tool and the soil, with the rotary blade defined as the master contact surface and all SPH particles in the soil model as the slave contact surface; The \*PART keyword is used to define the tool as the contact part and the soil as the target part, and to associate the soil material, model and algorithm; Constraints are applied to the bottom and lateral SPH particles of the soil model using the \*BOUNDARY\_SPC\_SET keyword; The \*BOUNDARY\_PRESCRIBED\_MOTION\_RIGID keyword is used to set the tool's forward speed to 0.3 m/s and rotational speed to 0.22 rad/s. Finally, the SPH simulation model of the soil-tool interaction is established, as shown in Figure 9.

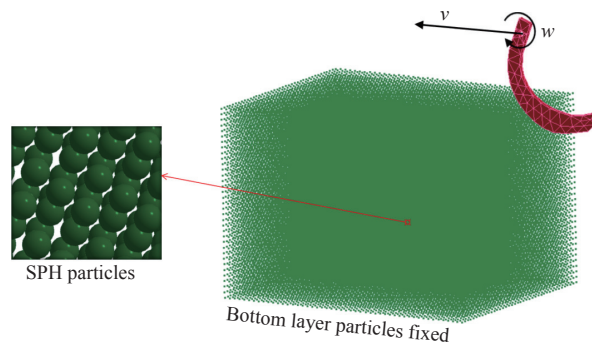


Figure 9 Simulation model of tool-soil interaction

**2.5 Response surface optimization methods**

During the design process of the rotary blade, three critical parameters in the structural design, namely the rake angle of the bend point, the direction angle of the side cutting edge bend line, and the bend angle, have a significant impact on the working performance of the rotary blade<sup>[31]</sup>. Therefore, these three design parameters denoted as  $X_1$ ,  $X_2$ , and  $X_3$ , were chosen as the controlled factors in the experimental design. A three-factor, five-level quadratic orthogonal rotating experiment was designed, and the response surface optimization experiment was conducted using the Box-Behnken Design method. The cutting power consumption ( $Y$ ) was selected as the optimization indicator for the simulation experiments. The coding levels of the experimental factors are listed in Table 3, and the results of the simulation experiments are listed in Table 4.

**Table 3 Coding level table of test factors**

Coding	Factors		
	Bend Point Wrap Corner $X_1$ /(°)	Directional angle of side cutting edge bending line $X_2$ /(°)	Bending corners $X_3$ /(°)
1.682	30.73	52.49	126.22
1	29.22	51.48	123.70
0	27.00	50.00	120.00
-1	24.78	48.52	116.30
-1.682	23.27	47.51	113.78

**3 Results and analysis**

**3.1 Simulation results and analysis**

During cutting, the side cutting edge of the tool comes into contact with the soil. The SPH particles of the soil in this region move along with the side cutting edge, and at this stage, the soil is not yet broken or loosened. As the cutting time increases, the contact between the tool and the soil intensifies, increasing in shear

**Table 4 Summary of simulation test results**

No.	$X_1$	$X_2$	$X_3$	Energy consumption for soil cutting $Y$
1	1	1	1	0.239
2	1	1	-1	0.289
3	1	-1	1	0.348
4	1	-1	-1	0.364
5	-1	1	1	0.359
6	-1	1	-1	0.511
7	-1	-1	1	0.432
8	-1	-1	-1	0.49
9	1.682	0	0	0.181
10	-1.682	0	0	0.398
11	0	1.682	0	0.384
12	0	-1.682	0	0.537
13	0	0	1.682	0.389
14	0	0	-1.682	0.511
15	0	0	0	0.446
16	0	0	0	0.446
17	0	0	0	0.446
18	0	0	0	0.446
19	0	0	0	0.446
20	0	0	0	0.446

and compressive forces exerted on the soil. This leads to crushing and dispersion of the soil along the cutting edge, causing significant deformation and damage to the soil layers. The motion and stress variations of the SPH soil particles when the tool first contacts the soil during the cutting process are shown in Figure 10.

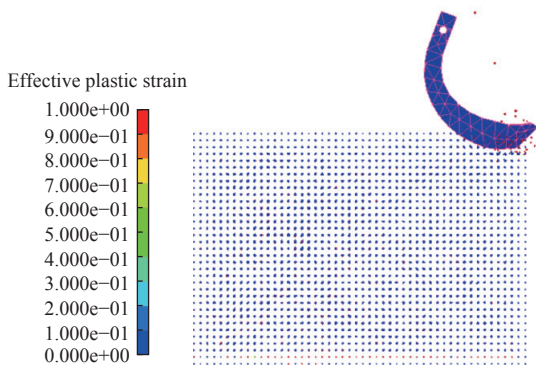
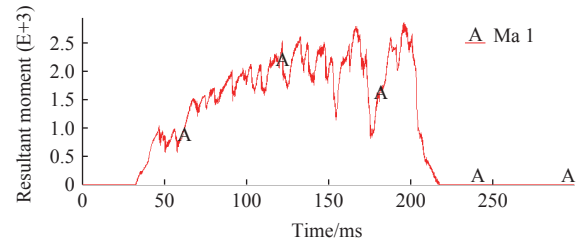


Figure 10 Stress changes during soil cutting simulation

Cutting force refers to the force required to deform the soil during the cultivation process of the tool. On the other hand, cutting resistance refers to the force exerted on the rotary tiller by the soil it is working on<sup>[31]</sup>. Using the LS-DYNA solver, the tool’s variation curve of cutting force is obtained, as shown in Figure 11. The cutting force of the tool during cutting increases gradually to reach the maximum value and then decreases rapidly, and the change rule of the cutting force is consistent with the changing trend of the cutting force obtained from the simulation of rotary tillage knives cutting soil by Fang et al.<sup>[32]</sup> using the discrete element method, and Shi<sup>[33]</sup> using the finite element (Display Dynamics) method, which verifies the feasibility and accuracy of this SPH simulation for simulating the tillage of the tool.

After analysis in the first cutting cycle, the cutting depth increases continuously as the tool gradually comes into contact with the soil. Numerous soil particles experience compression and friction, resulting in increasing soil resistance. The cutting force starts from zero and gradually increases. Between 50-100 ms, the cutting resistance increases the fastest, reaching its maximum value,

and then fluctuates within a specific range. As the rotary blade gradually disengages from the soil, the cutting force rapidly decreases until it reaches zero, indicating that it is entirely free from the soil.



Note: Ma 1 in the legend means the changing curve is obtained by simulating under Mach number is 1.

Figure 11 Cutting force curve during cutting

Cutting energy consumption in soil includes the energy expended in soil fragmentation (internal energy) and the energy consumed by the motion of the rotary tiller itself. In the energy curve shown in the simulation results, the total cutting energy (Total Energy) is obtained by combining the kinetic energy time history curve and the internal energy time history curve, as shown in Figure 12.

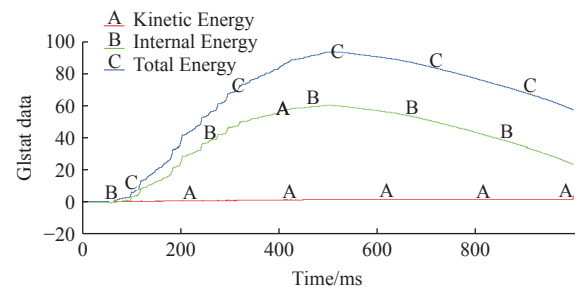


Figure 12 Energy curve of the cutting process

The tool itself has kinetic energy, which remains essentially unchanged compared to the change in internal energy during soil cutting, as shown by curve A in Figure 12. Therefore, the total energy change in soil cutting is consistent with the internal energy (energy consumed to break up the soil), as shown by curves B and C in Figure 12.

The analysis concluded that the cutting energy change rule is consistent with the actual cutting behavior, which is specifically shown in the rotary tillage knife gradually entering and cutting the soil in depth stage, the soil cutting volume and soil particle displacement continue to increase, the cutting energy is also slowly increasing, with the many soil particles are constantly squeezed and friction, driven forward and around the movement of the system energy continues to accumulate. When the rotary tillage knife is ready to leave the soil, the cutting energy reaches the maximum value, and then the contact area between the knife and the soil as well as the amount of soil cutting gradually decreases, and the energy required to break the soil gradually decreases.

**3.2 Field trials**

Field rotary tillage experiments were conducted in crop fields in Shihezi, Xinjiang. The average soil firmness was measured to be 2.16 MPa, and the moisture content was 10.64%. The experiments were carried out using a TN654 tractor equipped with the following devices: a rotary tillage unit, a mechanical tachometer (with a range of 0-400 r/min), and the NJTY3 agricultural machinery universal dynamic telemetry system, as shown in Figure 13. The power consumption was measured using wireless telemetry technology<sup>[34]</sup>,

employing a torque sensor integrated with the power output shaft and a frameless three-point hitch force sensor.



Figure 13 Field rotary cultivation test

Due to the complex situation in the field, the experimental results were unstable, so the power consumption within the specified time under the three tests was recorded, and the average value was taken as the experimental measurement results. Under the same initial simulation parameters (i.e.,  $X_1=27^\circ$  for the bend angle,  $X_2=50^\circ$  for the side cutting edge bend line direction angle, and  $X_3=120^\circ$  for the bend angle), the actual power consumption of individual rotary blade was measured and calculated as 0.21 kW. The measurement yielded a 7.1% error compared to the simulated power consumption of 0.195 kW. The results further validate the accuracy of the simulation. It is worth noting that the measured values are consistently higher than the simulated values, this rule is consistent with the results of other scholars in the test of soil cutting<sup>[35,36]</sup>.

The generation of such differences and patterns may stem from various factors, including variations in soil characteristics and structure, friction and wear of farming equipment, and levels of operational skills. The actual conditions of the soil may not align with the assumptions made in the simulation. For instance, soil properties in real-life scenarios may vary due to factors such as density, moisture content, and looseness, which could result in discrepancies between actual farming outcomes and simulations. Additionally, equipment wear and lack of regular maintenance may lead to a decline in the performance of tillage blades, further increasing energy consumption and resistance, factors typically not accounted for in simulation models. Furthermore, simulation models often assume stable and ideal operating parameters such as speed and depth. However, in real-world scenarios, the skill level and operational habits of the operator may also influence tillage effectiveness, resulting in disparities between actual results and simulated outcomes. Moreover, during actual operation, additional energy consumption may occur due to factors such as friction and wear caused by debris such as plant roots and gravel, apart from the soil, which contributes to actual tillage energy consumption and resistance being greater than simulated counterparts. Therefore, conducting in-depth analysis and discussion of these factors based on experimental results can help in better understanding the variations during the tillage process, enabling the refinement of simulation models and the provision of more effective solutions and optimizations for agricultural production.

### 3.3 Response surface optimization

#### 3.3.1 Optimization results and analysis

The power optimization based on the design parameters utilizes the Box-Behnken Design response surface optimization method. Using the ANOVA analysis feature in Design-Expert 12.0 software, predicted values for the regression model coefficients and the goodness of fit of the regression model equation can be obtained.

The F-test on the bending point included angle, side cutting edge bending line direction angle, and bending angle concerning the optimization target results in the regression model equation for cutting power consumption ( $Y$ ) as follows:

$$Y = -23.42629 + 0.606247X_1 + 0.403193X_2 + 0.119976X_3 - 0.005022X_1X_2 + 0.002191X_1X_3 - 0.002922X_2X_3 - 0.012007X_1^2 + 0.000586X_2^2 - 0.000177X_3^2 \quad (10)$$

The results of variance analysis and significance tests on the regression model are shown in Table 5. The variance analysis results indicate that the model has a significance level of  $p < 0.0001$ , indicating the significant influence of the three factors on cutting power consumption. Among them, the bending point included angle ( $X_1$ ) has the most significant impact on the cutting power consumption of the rotary tiller blade, while the interaction terms  $X_1X_2$  also have essential effects on power consumption. The significance of each factor on resistance can be determined based on the magnitude of the regression coefficients for each factor in the model. Their impact on cutting power consumption of the rotary tiller blade on the soil is in a descending order as:  $X_1$ ,  $X_2$  and  $X_3$ .

Table 5 Analysis of variance and significance test table

Source of variance	Sum of squares	Freedom	Mean square	F value	p value	Importance level
model	0.1545	9	0.0172	70.55	<0.0001	--
$X_1$	0.0616	1	0.0616	253.04	<0.0001	**
$X_2$	0.0178	1	0.0178	73.24	<0.0001	**
$X_3$	0.0170	1	0.0170	69.68	<0.0001	**
$X_1X_2$	0.0022	1	0.0022	8.95	0.0135	**
$X_1X_3$	0.0026	1	0.0026	10.65	0.0085	--
$X_2X_3$	0.0020	1	0.0020	8.42	0.0158	--
$X_1^2$	0.0505	1	0.0505	207.40	<0.0001	**
$X_2^2$	0.0000	1	0.0000	0.0976	0.7611	--
$X_3^2$	0.0001	1	0.0001	0.3493	0.5676	--
Residual error	0.0024	10	0.0002	--	--	--

Note: \* indicates significant ( $p < 0.05$ ), \*\* indicates highly significant ( $p < 0.01$ )

The parameter optimization of the rotary tiller blade based on the response surface method in this study resulted in the quadratic regression model (7), which provides the interaction response surfaces between pairs of factors. These surfaces are depicted in Figure 14.

Using the optimization feature and considering the actual operating conditions of the rotary tiller blade, as well as the roundness of the design parameters for practical manufacturing, the response surface method was applied for analysis. Considering actual production requirements, the optimal parameters were determined to be a bend point included angle of  $30^\circ$ , a lateral cutting edge bend line angle of  $51^\circ$ , and a bending angle of  $120^\circ$ . The corresponding optimal power consumption was found to be 0.181 kW.

The optimized parameters were reutilized to model the rotary tiller, maintaining consistency with the initial simulation parameters such as boundary conditions. Subsequently, a cutting simulation experiment was conducted again. The simulated power consumption was measured at 0.184 kW, indicating a reduction of 5.64% compared to the initial simulation result of 0.195 kW. This validates the effectiveness of the parameter optimization in reducing soil cutting power consumption.

After conducting field tests with the optimally designed parameters for the rotary cultivator, the measured actual

power consumption was found to be 0.19 kW, which is a 9.52% reduction compared to the initial power consumption. The results show that the energy consumption of soil cutting is effectively and practically reduced by the optimization of structural parameters of rotary blade.

3.3.2 Structural statics finite element simulation

Finite element evaluation was conducted simultaneously by applying a force of 500 N perpendicular to the surface at the locations of the lateral cutting edge, tangential cutting edge, and

transition edge of the rotary tiller blade. The equivalent stress was added, and the simulation results were obtained, as shown in Figure 15a. The maximum stress value was 181.52 MPa, occurring at the connection between the back curve and the blade handle. Total deformation was added, and the simulation results were obtained, as shown in Figure 15b. The maximum displacement deformation of the rotary tiller was 1.2133 mm, occurring at the tangential edge. These calculation results all comply with the mechanical requirements of the rotary blade.

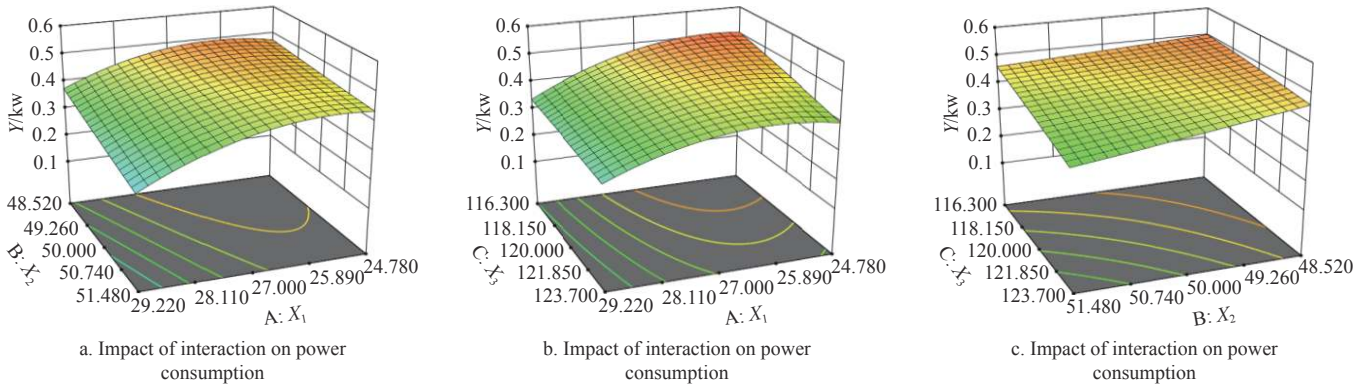


Figure 14 Interaction response surface of various factors

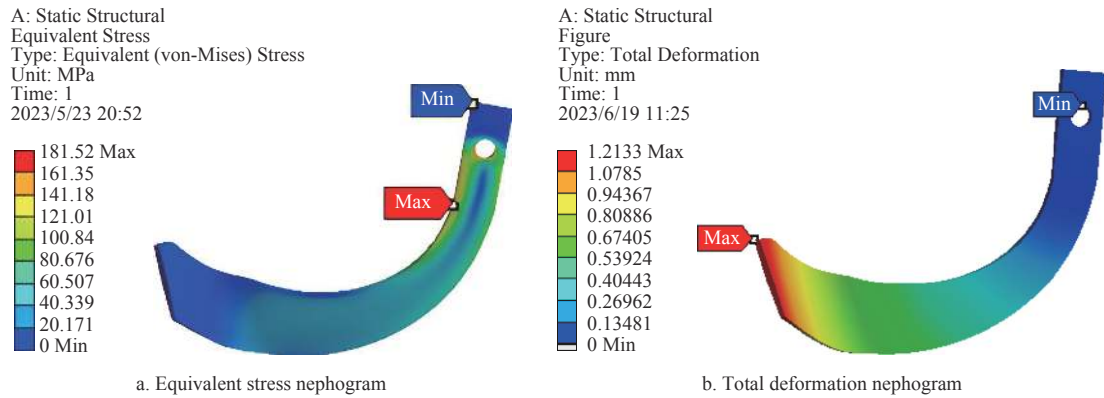


Figure 15 FEM simulation results

4 Conclusions

This study used a mesh-free SPH method to simulate soil cutting with a rotary tillage blade. The principles and modelling process of the SPH method are explained in detail. A high-precision soil-blade interaction model is established to investigate cutting phenomena, such as soil particle behavior and cutting resistance. The study also focuses on optimizing the cutting energy based on structural parameters while considering the impact of the blade's structural performance. The ultimate goal is to achieve an optimized blade design that minimizes cutting energy consumption. The following conclusions are obtained from the research:

- 1) Starting from the design and motion analysis of rotary tiller blades, this study highlights the advantages and limitations of the Smoothed Particle Hydrodynamics (SPH) method in simulating soil tillage compared to other simulation methods. It elaborates on the basic principles and processes of simulating soil cutting with SPH, emphasizing dynamic simulations to obtain information such as soil stress and tillage power consumption, thereby revealing cutting patterns. Simulation results indicate a deviation of 7.1% compared to actual power consumption, validating the accuracy of SPH method in simulating rotary tiller soil cutting.
- 2) A simulation experiment was designed for the rotary tillage

blade to perform orthogonal rotating combination tests in soil cutting. The objective of the experiment was to minimize power consumption. Based on the structural parameters, optimization was carried out using the response surface methodology while considering practical production constraints. The optimal parameters were determined as a bend point included angle of 30°, a side cutting edge bending line direction angle of 51°, and a bend angle of 120°. The optimized power consumption achieved was 0.181 kW. With the optimized parameters, the rotary blade was tested again in field experiments, and the measured power consumption was found to be 0.19 kW. This represents a 9.52% reduction in power consumption compared to the initial value. The optimization of the blade design has effectively reduced the power consumption in soil cutting.

- 3) The structural simulation of the optimized rotary tillage blade revealed that the stresses and strains in the blade holder, handle, and lateral cutting section were relatively small. The maximum stress in the rotary tillage blade was measured to be 181.52 MPa, located in the upper part of the back curve. The maximum displacement deformation value was 1.2133 mm, at the tangent edge. Furthermore, the distribution of stresses and strains was not concentrated in a specific region, indicating that the computed results meet the requirements of structural mechanics.

These findings provide a theoretical basis for optimizing the design parameters of the rotary blade.

## Acknowledgements

This work was supported by the National Key R & D Program of China - Science and Technology Innovation 2030 New Generation Artificial Intelligence (Grant No. 2022ZD0115804), the Major Science and Technology Projects in Xinjiang Uygur Autonomous Region (Grant No. 2022A02012-4) and the Construction Project of Demonstration Platform for National New Materials Production & Application (Grant No. TC200H01X-5).

## [References]

- [1] Yuan Y W, Bai S H, Niu K, Zhou L M, Zhao B, Wei L G, et al. Research progress on key technologies and equipment of mechanization in cotton planting. *Transactions of the CSAE*, 2023; 39(6): 1–11. (in Chinese)
- [2] Mottaleb K A, Rahut D B, Ali A, Gérard B, Erenstein O. Enhancing smallholder access to agricultural machinery services: lessons from Bangladesh. *The Journal of Development Studies*, 2017; 53: 1502–1517.
- [3] Cui S Y, Zhu X K, Cao G Q. Effects of tillage on soil nitrogen and its components from rice-wheat fields in subtropical regions of China. *Int J Agric & Biol Eng*, 2022; 15(3): 146–152.
- [4] Han Q C, Ren A M, Zhang Y J, Yi G, Cui M J, Zhang J J, et al. The impact of various cultivation techniques on cotton growth and development. *Hebei Agricultural Sciences*, 2014; 18(2): 7–9, 21. (in Chinese)
- [5] Liu D W, Xie F P, Ye Q, Ren S G, Li X, Liu Z M. Analysis and experimental study on influencing factors of power consumption of trenching components for 1K-50 orchard trenching machine. *Transactions of the CSAE*, 2019; 35(18): 19–28. (in Chinese)
- [6] Godwin R J, O'Dogherty M J, Saunders C, Balafoutis A T. A force prediction model for mouldboard ploughs incorporating the effects of soil characteristic properties, plough geometric factors and ploughing speed. *Biosystems Engineering*, 2007; 97: 117–129.
- [7] Zhang G W. Application of Digital Design Technology in Agricultural Machinery Design. *Agricultural Technology and Equipment*, 2019; 21: 14–16. (in Chinese)
- [8] Jia H L, Wang W P, Chen Z, Zheng T Z, Zhang P, Zhang J. Current status and prospect of optimization research on tillage components of agricultural machinery. *Transactions of the CSAE*, 2017; 48(7): 1–13. (in Chinese)
- [9] Gao T, Xie S Y, Hu M, Tan Q T, Fang H Z, Yi C, Bao A H. Soil-soil component SPH interaction model based on sub plastic constitutive model. *Transactions of the CSAE*, 2022; 38: 47–55. (in Chinese)
- [10] Li X, Zhu L, Gong S. Soil-cutting simulation and dual-objective optimization on tillage process parameters of micro-tiller by smoothed particle Galerkin modeling and genetic algorithm. *Computers and Electronics in Agriculture*, 2022; 198: 107021. DOI
- [11] Sun H. Simulation and experiment of soil cutting process of orchard trenching tool based on SPH algorithm. *Journal of Chinese Agricultural Mechanization*, 2019; 40: 190–194. (in Chinese)
- [12] Hu M, Gao T, Dong X, Tan Q T, Yi C, Wu F, Bao A H. Simulation of soil-tool interaction using smoothed particle hydrodynamics (SPH). *Soil & Tillage Research*, 2023; 229: 105671.
- [13] Li S T, Chen X B, Chen W, Zhu S W, Li Y W, Yang L, et al. Soil-cutting simulation and parameter optimization of handheld tiller's rotary blade by smoothed particle hydrodynamics modelling and Taguchi method. *Journal of Cleaner Production*, 2018; 179: 55–62.
- [14] Niu P. Research on power consumption and vibration characteristics of electric micro tiller. Doctoral dissertation. Chongqing: Southwest University, 2020; 126p. (in Chinese)
- [15] Guan C S, Fu J J, Xu L, Jiang X Z, Wang S L, Cui Z C. Study on the reduction of soil adhesion and tillage force of bionic cutter teeth in secondary soil crushing. *Biosystems Engineering*, 2022; 213: 133–147.
- [16] Xiao M H, Niu Y, Wang K X, Zhu Y J, Zhou J F, Ma R Q. Design of self-excited vibrating rotary cultivator and analysis of torque reduction and energy saving performance. *Transactions of the CSAM*, 2022; 53(11): 52–63. (in Chinese)
- [17] Sun Z, Duan J L, Yang Z. Research progress on the technology of rotary tillage for reducing drag and energy consumption. *Journal of Chinese Agricultural Mechanization*, 2021; 42(1): 37–45. (in Chinese)
- [18] Hao Z H, Zheng E L, Li X, et al. Analysis of tillage performance and structural optimization of no-tillage seeder rotary cultivator. *Transactions of CASE*, 2023; 39(2): 1–13. (in Chinese)
- [19] Jin X M, Ma F P, Wang D, Zhu Z T. Simulation of mouldboard plough soil cutting based on smooth particle hydrodynamics method and FEM-SPH coupling method. *Agriculture*, 2023; 13(9): 1847.
- [20] Zhang X Y, Zhang L X, Hu X, Wang H, Shi X B, Ma X. Simulation of soil cutting and power consumption optimization of a typical rotary tillage soil blade. *Applied Sciences*, 2022; 12: 8177.
- [21] Wang X Z, Li P, He J P, Wei W Q, Huang Y X. Discrete element simulations and experiments of soil-winged subsoiler interaction. *Int J Agric & Biol Eng*, 2021; 14(1): 50–62.
- [22] Ma C, Meng H W, Zhang J, Zhang Z, Zhao Y, Wang L H. Research and experiment on the trenching performance of orchard trenching device. *Scientific Reports*, 2023; 13: 18941.
- [23] GB/T 5669-2017. Rotary tiller - Rotary blades and blade holders. Beijing: China Standards Press, 2007. (in Chinese)
- [24] Li B F. *Agricultural mechanics*. China Agriculture Press, 2003; 438p. (in Chinese)
- [25] Fourtakas G, Rogers B D. Modelling multi-phase liquid-sediment scour and resuspension induced by rapid flows using Smoothed Particle Hydrodynamics (SPH) accelerated with a Graphics Processing Unit (GPU). *Advances in Water Resources*, 2016; 92: 186–199.
- [26] Fan C. Research on fluid simulation based on SPH method. Master's thesis. Hefei: Hefei University of Technology, 2017. (in Chinese)
- [27] Zhao Y Z, Ma Z B. Study on optimal selection and adaptive criterion of SPH kernel smooth length. *Computational Physics*, 2017; 34(1): 29–38.
- [28] Monaghan J J, Gingold R A. Shock simulation by the particle method SPH. *Journal of Computational Physics*, 1983; 52(2): 374–389.
- [29] Benz W. Applications of Smooth Particle Hydrodynamics (SPH) to astrophysical problems. *Computer Physics Communications*, 1988; 48(1): 97–105.
- [30] U. S. Department of Transportation Federal Highway Administration Evaluation of LS-DYNA soil material mode 147. Georgetown: Turner-Fairbank Highway Research Center, 2004.
- [31] Li S T. Design, optimization, and cutting performance study of rotary tiller blades for micro tiller. Master's thesis. Chongqing: Southwest University, 2018. (in Chinese)
- [32] Fang H M, Ji C Y, Zhang Q Y, Guo J. Force analysis of rotary cultivator based on discrete element method. *Transactions of CASE*, 2016; 32(21): 54–59. (in Chinese)
- [33] Shi X B. Numerical analysis of working process and friction wear of micro tiller plow knife. Master's thesis. Shihezi: Shihezi University, 2023. (in Chinese)
- [34] Kang J M, Li S J, Yang X J, Liu L J, Li C Y. Power consumption simulation analysis and test verification of disc trencher. *Transactions of CASE*, 2016; 32(12): 8–15. (in Chinese)
- [35] Zhang X Y, Zhang L X, Shan Y C, Wang H, Shi X B. Finite element simulation and optimization of key parameters for rotating tilling soil-engaging components. *Agricultural Mechanization Research*, 2023; 45(11): 36–42.
- [36] Liu J A. Optimization of deep loosening shovel parameters and comprehensive effect of soil loosening based on discrete element method. Doctoral dissertation. Beijing: China Agricultural University, 2018. (in Chinese)